Chapter 3

Polythiophene-functionalized MWCNT Nanocomposites: Preparation and Properties

3.1. Introduction

Comprehensive knowledge of conducting polymers and carbon nanotubes available in the literature is beneficial for developing conducting nanocomposites of conducting polymers with carbon nanotubes. The critical parameters for such nano composite preparation include compatibility of component phases and changes in optoelectrical and mechanical properties.[1-10] However, the creation of nanocomposites confronts some technical difficulties also. The difficulty in improving the solubility or dispersibility of individual components in the reaction medium due to the hydrophobic nature of carbon nanotubes and conducting polymer is a significant obstacle for preparing nanocomposites.[10,11] Aggregation tendency of carbon nanotubes in bundled form is another factor that hinders the formation of dispersed CNTs for nanocomposites preparation.[6,10]

Suitable surface functionalization techniques can minimize the aggregation tendency of carbon nanotubes. The surface functionalization of carbon nanotubes can be carried out by a covalent or non-covalent approach. Small functional groups introduced to the surface of carbon nanotube can be further derivatised to larger chemical entities[12,13-15] or grafting of polymer on the surface of CNT through covalent bonding[16,17] or non-covalent orientation of small molecules on the surface of CNT[18,19] and non-covalent wrapping of polymer chains on CNT surface.[15,20] Different functionalization practices of carbon nanotubes are shown in **Figure 3.1.** Covalent attachment of hydrophilic functional groups is better practice than relatively weak non-covalent modification for providing higher solvent compatibility and strong interfacial interaction with other matrices in its composite state.[14,19,21] Excessive covalent functionalization or functionalization under harsh conditions could create good coverage of functional groups, however it might severely damage the intrinsic molecular structure of CNT and produce smaller carbonaceous fragments.[14,15,20] Therefore, covalent modification of CNT furnishing moderate degree of functionalization would be more preferable.[21-23] Non-covalent functionalization is an attractive method to cover a large area of carbon nanotubes by suitably orienting the molecular or polymer moieties by weak non-covalent interactions such as hydrogen bonding, π-π stacking interactions, van der Waals force of attraction, etc. Non-covalent functionalization strategy provide less firmness to composite framework than the

covalent method because of weak non-bonded forces of attraction between the components. [19,24] But the advantage of non-covalent method of functionalization is that it does not significantly destruct the π-conjugated network structure.[19,25]

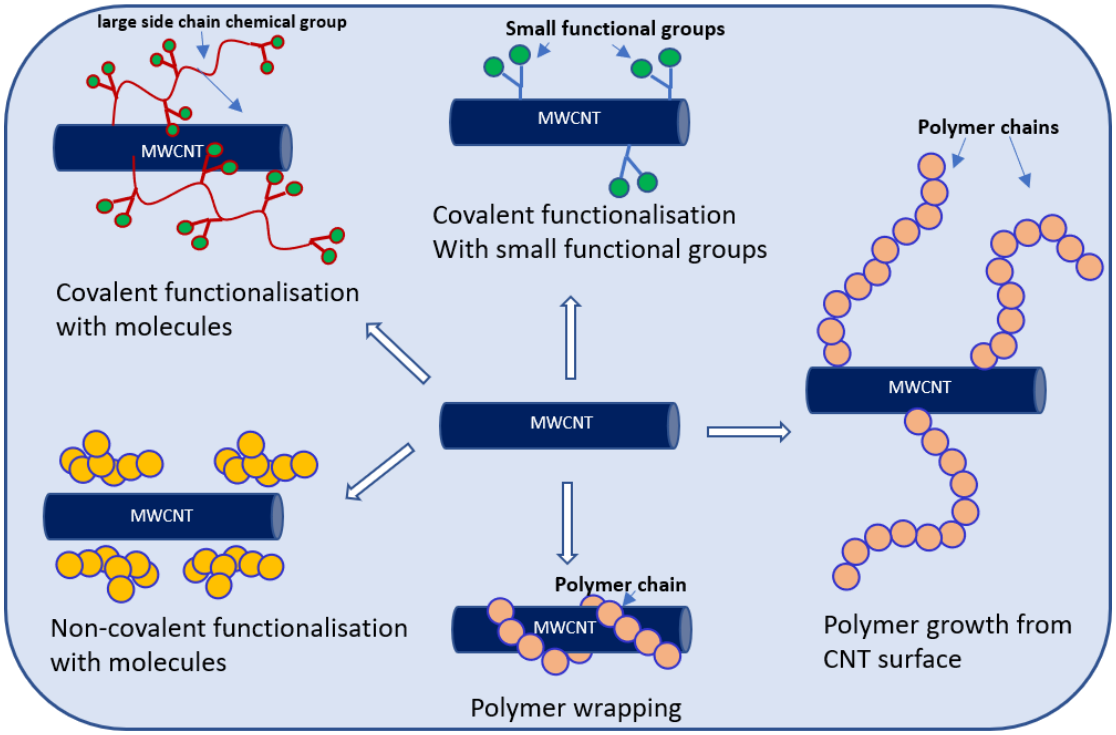

Figure 3.1. *Different surface functionalization strategies on carbon nanotubes.*

We could observe that covalent and non-covalent approaches to CNT functionalization impart their advantages and possess some limitations also. Hence, it would be more noteworthy to adopt the combined use of both covalent and non-covalent functionalization strategies for modifying carbon nanotubes. The strategy and protocol selected should be simple to execute and easy to be scaled up.[19,20,23,24,26] Yuan and Chan-Park reported that covalent combined with non-covalent functionalization of single-walled carbon nanotubes synergistically improved both carbon nanotube dispersion and nanotube phase transfer /matrix interfacial strength, leading to superior mechanical reinforcement in polymer nanocomposites (see **Figure 3.2. (1)**).[26] Clave et al. reported immobilisation of organic molecules in the internal hydrophobic cores of micelles followed by in-situ polymerisation around the nanotube scaffold. They adopted the combined use of covalent and non-covalent approaches for the specific modification of carbon nanotubes.[19] Berger and co-workers introduced a phase transfer method for polymer-wrapped single-walled carbon nanotubes to create luminescent

aryl defects. They proposed that the material as an efficient near-infrared light emitting diode as thin film (see **Figure 3.2. (2)**).[12] The combined use of covalent and non-covalent functionalization promoted solvent compatibility of the compound by minimizing the drawbacks arising from both the functionalization strategies.[12,19,26,27] In that way, mild covalent modification of CNT prior to non-covalent attachment of bulky conjugated polymer would be a better strategy to strengthen the interfacial interaction between the less destructed state of nanotubes and the polymer.[12,15,19]

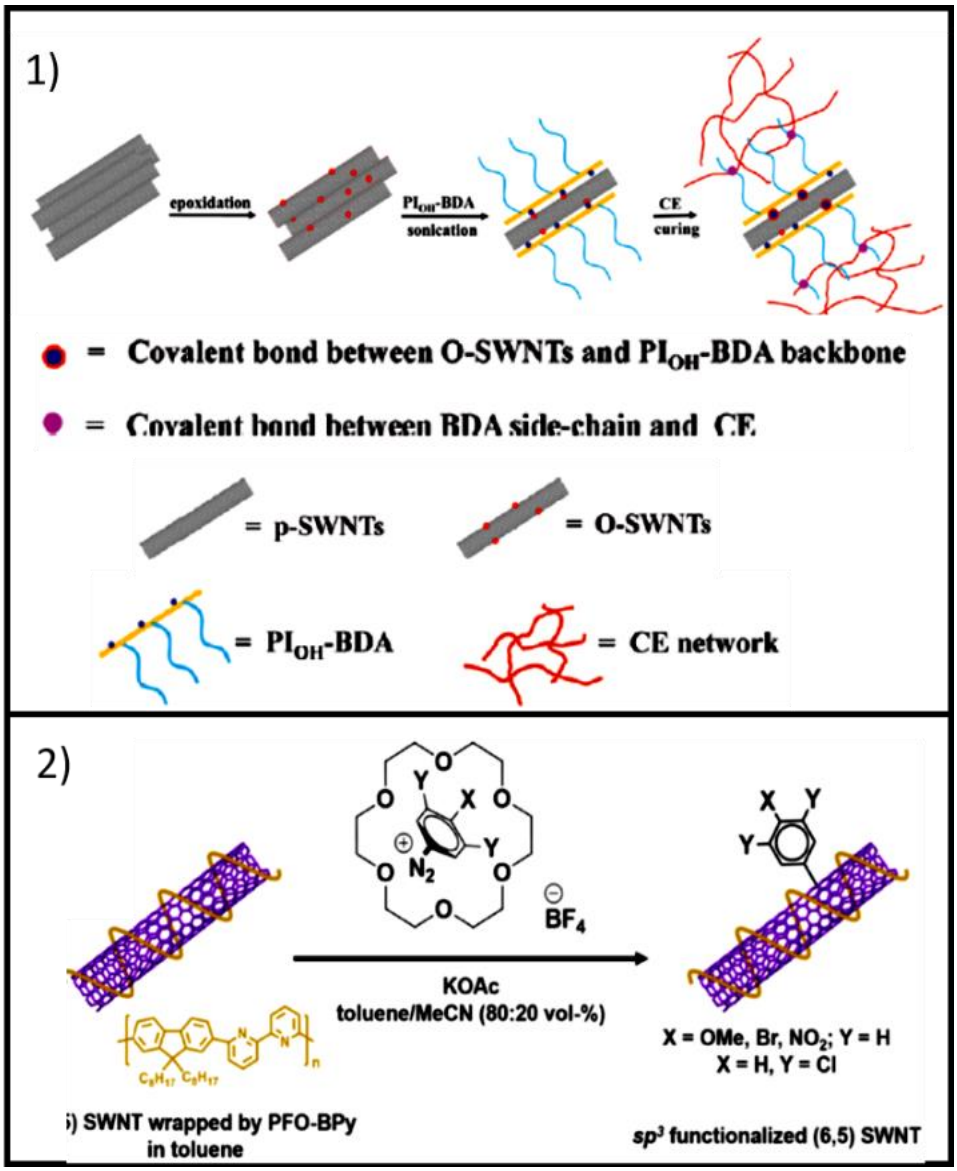

Figure 3.2. *Combined covalent cum non-covalent functionalization of carbon nanotubes with molecular and polymer entities adapted from 1)Yuan and Chan-Park 2012 and 2) Berger et al. 2019.*

Table 3.1. *Defect group functionalization and their relevance seen in the literature.*

Sl. no.	Method of functionalization	Defect group/s	Other materials incorporated	Relevance of work	Ref.
1	Electrochemical reduction	Aryl groups	-	Solubility enhancement, Switching and memory behaviour	28
2	Chemical (at 80-90°C)	Alkyl groups terminated with carboxylic acid groups and their extended amides	-	Large diamagnetic susceptibility based on theoretical study	29
3	Chemical	Carboxylic acid group	Polyvinyl alcohol	Polymer nanocomposite preparation	30
4	Free radical reaction	Alkyl groups and its derivatives	-	Improved solubility, high degree of functionalization	31
5	chemical	Carboxylic acid group	Different polymeric and oligomeric compounds	Enhanced solubility and strong luminescence emissions	32
6	Nitrogen glow discharge	C≡N group	-	Microwave generated nitrogen plasma as source of nitrogen containing functional groups	33
7	Chemical (argon ion treatment)	Free radical groups	-	Controlled functionalization using 2 ke V Ar^+	34
8	Chemical	Carboxylic acid groups	Derivatized polyimide	Nanocomposite formation with higher dispersibility	35
9	chemical	amine	-	Improved CO_2 adsorption	23
10	chemical	Carboxylic acid group	Polyvinyl alcohol	Increase in mechanical strength	36
11	Microwave excited Ar/O_2 surface wave plasma treatment	Oxygen containing functional groups	-	Good dispersion in water	37
12	Chemical	Carboxylic acid groups	polythiophene	Bilayer photovoltaics	9
13	Chemical (Hydrothermal oxidation)	Oxygen functional groups	-	Studied advantages of nitric acid oxidation	39
14	Chemical	Amide groups having phenolic linker	Single chain variable fragment protein	Detection of prostate cancer	38

Insertion of functional groups on the surface of CNT helps to improve its disentanglement and solvent compatibility in polar solvents.[31,32,39] Some of the defect group functionalization approaches selected from the literature and their relevance are summarised in **Table 3.1.** The tabulated data showed that functionalized carbon nanotubes, independently and in a composite state, have their own relevance in terms of property enhancement or in suitable applications.[9,23,28-39] Carboxylic acid groups and other oxygen-containing functional groups could be inserted on the CNT surface by adopting simple acid treatment methods. Here the polar nature of such defect functional groups can facilitate the formation of dispersible carbon nanotubes in polar medium.[14,26] Acid treatment would be attractive as a simple functionalizing strategy without damaging the intrinsic chemical structure of CNT and enhancing the water dispersion by the involvement of hydrogen bonding between carboxylic acid functional groups and water molecules. Polymers or other structurally related molecules are usually being selected for further modifications in the acid-functionalized carbon nanotubes.[13,18,26] Polymer can be combined with functionalized CNT by covalent or non-covalent modification (see **Figure 3.3.**).[12,26,27]

In this chapter, carboxylic acid functionalization of multi-walled carbon nanotubes were carried out using oxidative treatment with HNO_3 followed by a non-covalent approach of nanocomposite preparation with conducting polythiophene in the presence of AOT surfactant. In effect, covalent functionalization followed by non-covalent modification was implemented here as a preparation strategy for nanocomposites. Defect group functionalization improved the non-covalent compatibility of carbon nanotubes with polythiophene matrix via enhancing non-covalent surface interactions. FT-IR and Raman spectra were recorded to analyse the acid functionalization of MWCNT. The MWCNT-COOH and PTCNT-COOH nanocomposites were characterized using FT-IR analysis, elemental analysis, X-ray photoelectron spectroscopy, X-ray diffraction analysis and pH measurements. Morphological analyses were also conducted with FE-SEM and HR-TEM imaging. UV-vis absorption spectra were recorded in the dispersed state of the nanocomposite in chloroform medium. Thermal stability and electrical conductivity were also measured. The chapter has given immense attention for describing the formation of polythiophene-functionalised MWCNT core-shell nanocomposite with enhanced electrical conductivity and thermal stability.

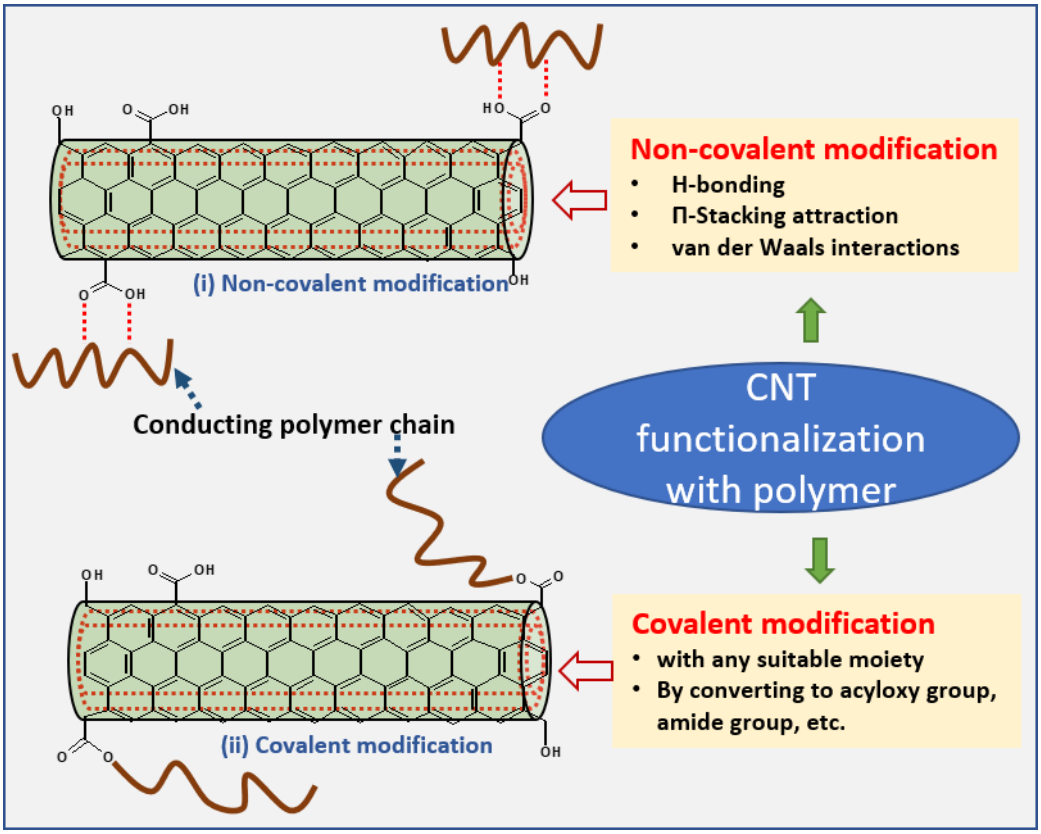

Figure 3.3. *Non-covalent functionalization (modification) and covalent functionalization (modification) of CNT with polymer.*

3.2. Experimental

3.2.1. Materials and reagents: Thiophene, ferric chloride, sodium bis (2- ethyl hexyl) sulfosuccinate (AOT) and multi-walled carbon nanotubes were purchased from Sigma Aldrich and used without further purification. Deionized water, conc. HNO_3, chloroform and acetone were purchased from Merck chemicals, India.

3.2.2. Measurements and instruments: FT-IR spectra of the samples were recorded using KBr pellet method by Shimadzu IR Affinity 1 spectrometer. The elemental analyses (CHNS) of the samples were carried out using elementar vario EL III element analyser. Powder X-ray diffraction (P-XRD) analyses of the samples were conducted using PANALYTICAL, Aeris research with 2θ values ranging from 5°-90°. pH studies were carried out with HM digital PH-80 Temp hydrotester. Scanning electron microscopic (SEM) imaging were conducted using JEOL Model JSM-6390LV scanning electron microscope. Transmission electron microscopic (TEM) images were

recorded with JEOL/JEM 2100 instrument having a capacity of 200 KV with magnification 2000x-1500000x. Electrical conductivity of the samples were measured using DFP-RM-200 with constant current source Model CCS-01 and DC microvoltmeter. UV-visible absorption spectra of the samples were recorded with HPLC grade chloroform and double deionized water as solvent using Shimadzu UV-Visible spectrophotometer 1800 series. Thermogravimetric analysis (TGA) was carried out using Perkin Elmer, Diamond TG/DTA.

3.2.3. Synthesis of MWCNT-COOH 5M: MWCNT (0.40 g) was added to nitric acid (5 M, 50 mL) taken in an RB flask and then sonicated for 15 min for making dispersion. The reaction mixture was refluxed at 100 ºC for 7 h with magnetic stirring. The refluxed reaction mixture was washed with deionized water until the pH of the filtrate became neutral. This was then washed with acetone, filtered and dried in vacuum oven at 60º C for 3 h. Yield: 0.36 g. FT-IR (KBr, cm^{-1}) 1465, 1504, 1648, 1698, 1741.

3.2.4. Synthesis of PTCNT-COOH 300: Monomer thiophene (1 mL, 12.50 mmol) and surfactant AOT (0.22 g, 0.50 mmol) was dissolved in chloroform (20 mL) and sonicated for 5 min. MWCNT-COOH (0.30 g) was added to the AOT-thiophene mixture in chloroform and sonicated for 10 min. The dispersed form of $FeCl_3$ in 10 mL chloroform was added drop by drop to the AOT-thiophene-MWCNT-COOH mixture and then sonicated for 15 min. Subsequently, the reaction mixture was magnetically stirred for 3 h. Polymer nanocomposite thus obtained was filtered and washed using water and acetone. The resultant composite was then dried in a vacuum oven at 60°C. Yield: 0.82 g. FT-IR (KBr, cm^{-1}) 1667, 1536, 1028 (w), 779 (w), 668. Elemental analysis (anal., wt %): C, 41.14; S, 17.80; H, 3.02.

PTCNT-COOH 100 and PTCNT-COOH 200 were prepared using the same procedure as above by changing the quantity of MWCNT to 0.10 and 0.20 g, respectively. The figures mentioned in sample codes PTCNT-COOH 100, PTCNT-COOH 200 and PTCNT-COOH 300 represent the amount of multi-walled carbon nanotubes used in milligrams for the preparation of respective nanocomposites. Preparation of PTCNT-COOH 100 and PTCNT-COOH 200 yielded 1.16 g and 1.22 g of nanocomposites, respectively.

3.2.5. Synthesis of PT2CNT-COOH 300: Monomer thiophene (0.5 mL, 6.25 mmol) and AOT (0.11 g, 0.25 mmol) were dissolved in chloroform (10 mL) and sonicated for

5 min. To the monomer-AOT solution mixture, MWCNT-COOH (0.075 g) was added and sonicated for 10 min. Ferric chloride (1.22 g, 7.50 mmol) dispersed in 5 mL chloroform was added drop by drop to monomer-surfactant-MWCNT mixture and sonicated for 15 min. After that, it was stirred using a magnetic stirrer for 3 h. The resultant polymer-nano composites were washed using water and acetone and finally filtered by suction pump. The composite obtained was dried in vacuum oven at 60ºC for 3 h. Yield: 0.193 g.

PT3CNT-COOH-300 was prepared using the same procedure by changing the amount of thiophene to 0.75 mL (9.36 mmol). The yield obtained for PT3CNT-COOH 300 was 0.278 g.

3.3. Results and Discussion

3.3.1. Synthesis and characterization of functionalized MWCNT-COOHs

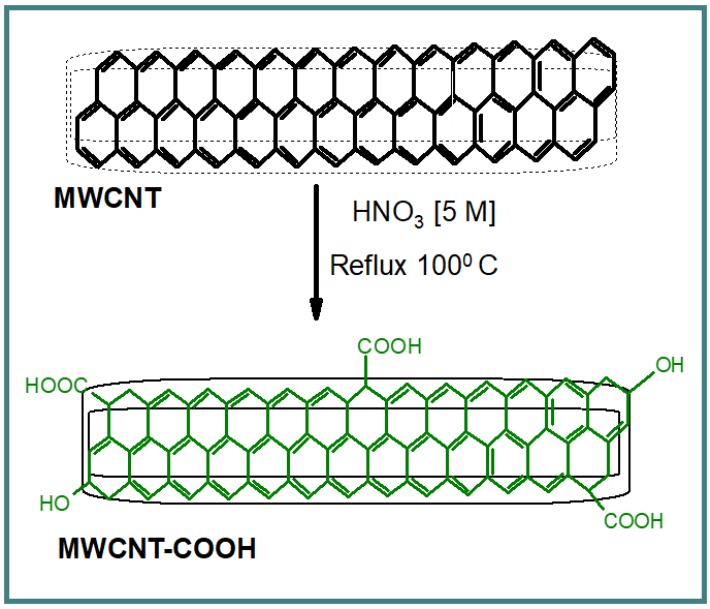

Figure 3.4. *Schematic representation of the preparation of MWCNT-COOH*

Carboxylic acid-functionalized multi-walled carbon nanotubes were prepared by refluxing MWCNT with nitric acid at 100°C for 7 h. Different reagent conditions adopted for acid functionalization involve treatment with 5 M HNO_3, 10 M HNO_3, and combined use of 5 M HNO_3 along with $NaNO_3$, producing functionalized MWCNTs named MWCNT-COOH 5M, MWCNT-COOH 10M and MWCNT-COOH-N 5M respectively. Treatment with nitric acid creates defective sites on the walls of carbon nanotubes and produce different functional groups like

carboxylic acid, hydroxyl group, aldehyde and keto group, etc.[25] Inherent agglomeration tendency of carbon nanotubes always hinders the processability in applications. Literature studies reveals that the acid functionalization of carbon nanotubes is an uncomplicated and cost-effective way to improve the dispersion in polar solvents.[14,25] Schematic representation of the synthesis of MWCNT-COOH 5M is given in **Figure 3.4.**

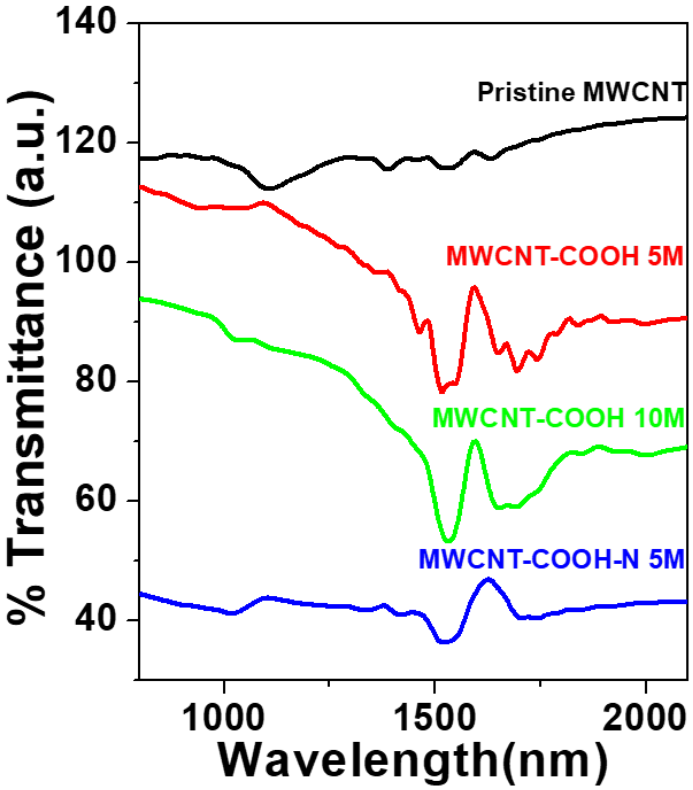

Figure 3.5. *FT-IR spectra of Pristine MWCNT, MWCNT-COOH 5M, MWCNT-COOH 10M and MWCNT-COOH-N 5M*

Structural changes on the walls of multi-walled carbon nanotubes were studied by fourier transform infrared spectroscopy by making thin pellets of samples with KBr powder. FT-IR spectra of pristine MWCNT, MWCNT-COOH 5M, MWCNT-COOH 10M and MWCNT-COOH-N 5M are shown in **Figure 3.5.** Pristine MWCNTs have shown characteristic peaks at 1528 and 1641 cm^{-1} due to in-plane vibrations of graphitic walls of carbon nanotubes and C=C stretching vibrations of carbon nanotubes, respectively.[40,41] Good symmetry of the carbon nanotube produces weak dipole moment changes and hence poor signals.[42] MWCNT-COOH 5M, MWCNT-COOH 10M and MWCNT-COOH-N 5M exhibited strong infrared signals compared with pristine

MWCNT. Functionalized MWCNT-COOH samples showed peaks at 1465, 1528, 1648, 1698 and 1741cm^{-1} due to C-O bending of aliphatic alcohol, in-plane vibrations of graphitic walls, C=C stretching vibrations, C=O stretching vibrations of carbonyl (keto or aldehyde functional group) and carboxylic groups respectively.[41-43] The broad peaks corresponding to hydrogen-bonded -OH functional groups, including water molecules attached to CNT, were present in the range 3612 - 3744cm^{-1}.[43] The above outcomes indicated that the chemical treatment with HNO_3 produces defective sites functional groups on carbon nanotubes, including carboxylic acid groups. A comparison of the FT-IR spectra of MWCNT-COOH 5M, MWCNT-COOH 10M and MWCNT-COOH-N 5M suggested that MWCNT-COOH 5M exhibits good functionalization peaks with minimum use of nitric acid. Thereby MWCNT-COOH 5M was used for further preparations of polythiophene-MWCNT composites. The name MWCNT-COOH 5M is abbreviated as MWCNT-COOH for the remaining studies.

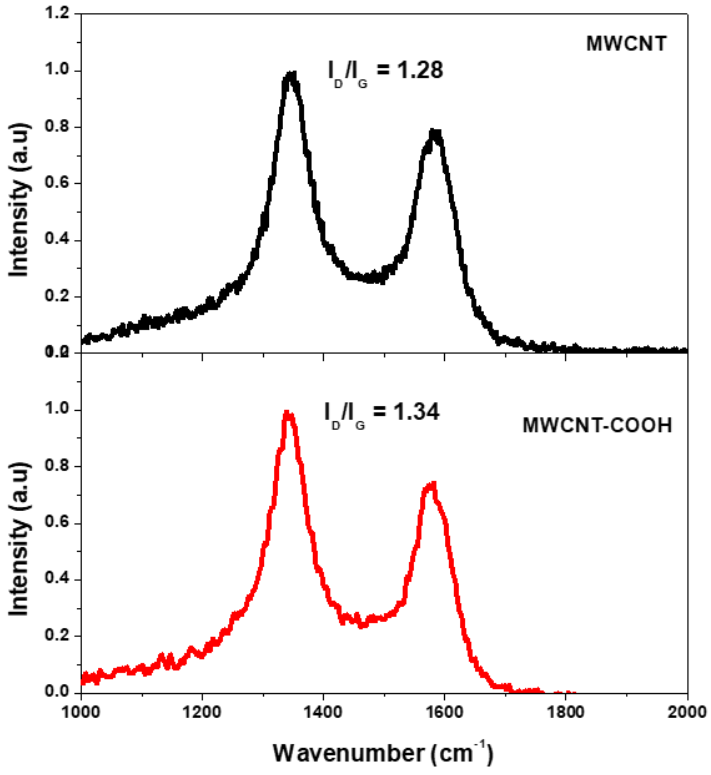

Figure 3.6. *Raman spectra of purified MWCNT and MWCNT-COOH*

Raman spectroscopy of purified MWCNT and functionalised MWCNT-COOH has been carried out to determine the degree of disorder in the graphitic structure of multi-walled carbon nanotube (see **Figure 3.6.**). Carbon nanotubes was purified by sonicating MWCNT with 0.5 M HNO_3 for 15 min followed by magnetic stirring for 30

min at room temperature. Pristine MWCNT may contain amorphous carbon and catalytic impurities, which could be removed with acid washing. The characteristic peaks of multi-walled carbon nanotube termed as G band and D-band were present at 1576 cm^{-1} and 1348 cm^{-1}, respectively. The G band was due to in-plane tangential stretching of the graphitic carbon-carbon bonds in graphene sheets and the D band was due to the presence of amorphous carbon and disordered structure in CNT.[41-43] The I_D/I_G ratio for purified MWCNT and functionalized MWCNT-COOH were found to be 1.28 and 1.34 respectively. The acid washing removes the impurities of pristine MWCNT, however, acid oxidation produced functionalization of carbon nanotube along with the removal of impurities, which resulted in a higher I_D/I_G ratio for functionalised MWCNT-COOH.[41,42]

3.3.2. Synthesis and characterization of PTCNT-COOH nanocomposites

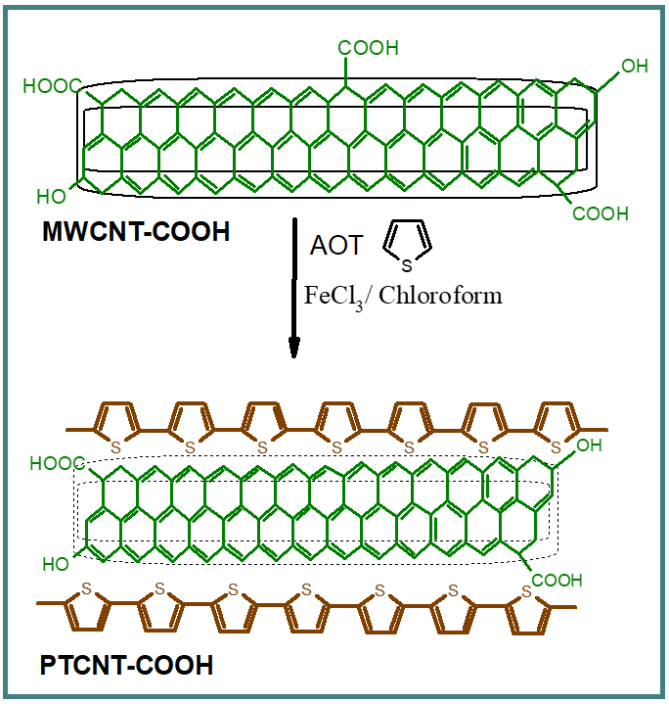

Figure 3.7. *Schematic representation of the synthesis of PTCNT-COOH nanocomposites.*

Polythiophene–functionalized multi-walled carbon nanotube nanocomposites (PTCNT-COOHs) were prepared by *in situ* oxidative chemical polymerization of thiophene monomer in the presence of functionalized multi-walled carbon nanotubes (MWCNT-COOH) using ferric chloride as the oxidizing agent and sodium bis(2-ethylhexyl) sulfosuccinate (AOT) as anionic surfactant. Thiophene-AOT micellar

complexes get attached to the walls of multi-walled carbon nanotubes through non-covalent interaction and get polymerized by oxidizing agents to result in water-dispersible core-shell nanostructured polythiophene-functionalized MWCNT-COOH nanocomposites.[44-47] The highly dispersed nature of MWCNT-COOH in $CHCl_3$ helps to orient thiophene-AOT micellar complexes near the locality of functionalized multi-walled carbon nanotubes, which in turn facilitates the polymerization of thiophene to take place quickly on the surface of multi-walled carbon nanotubes.[44] Scheme for the synthesis of PTCNT-COOH composite is represented in **Figure 3.7.** Details regarding the concentration of thiophene, AOT, and ferric chloride and the amount of MWCNT-COOH and the yield obtained were given in **Table 3.2.**

Table 3.2. *Millimoles of thiophene, AOT, and ferric chloride, amount of functionalized MWCNT-COOH, mole ratio of monomer/AOT, mole ratio of monomer/$FeCl_3$, elemental composition of samples and yield.*

Samples	**Thiophene (mmol)**	**AOT (mmol)**	**$FeCl_3$ (mmol)**	**MWCNT – COOH added (mg)**	**Monomer /AOT mole ratio**	**Monomer/ $FeCl_3$ mole ratio**	**Elemental Composition (%)**			**Yield (mg)**
							C	**H**	**S**	
PTCNT-COOH 100	12.50	0.50	15.00	100	1:1/25	1:1.2	61.52	0.41	26.72	490
PTCNT-COOH 200	12.50	0.50	15.00	200	1:1/25	1:1.2	-	-	-	600
PTCNT-COOH 300	12.50	0.50	15.00	300	1:1/25	1:1.2	66.58	0.31	17.53	700

The FT-IR spectroscopic studies of PT-25, pristine MWCNT, MWCNT-COOH and PTCNT-COOHs (100, 200 and 300) were carried out (see **Figure 3.8**.). The PT-25 has two major characteristic peaks that appeared at 787 and 688 cm^{-1} due to C-H out-of-plane deformation and C-S stretching of thiophene ring moiety.[48]. PTCNT-COOHs (100, 200 and 300) have shown well matched strong infrared signals with functionalized multi-walled carbon nanotubes (MWCNT-COOH). Functionalized MWCNT-COOH samples have shown peaks at 1465, 1528, 1648, 1698 and 1741cm^{-1} due to C-O bending of aliphatic alcohol, in-plane vibrations of graphitic walls, C=C stretching vibrations, C=O stretching vibrations of carbonyl (keto or aldehyde functional group) and carboxylic acid groups respectively.[41-43] PTCNT-COOHs

nanocomposites (100, 200 and 300) have the two extra peaks of polythiophene at 785 and 675 cm^{-1} corresponding to C-H out of plane deformation and C-S stretching of polythiophene chains in addition to the peaks in MWCNT-COOH.[48]

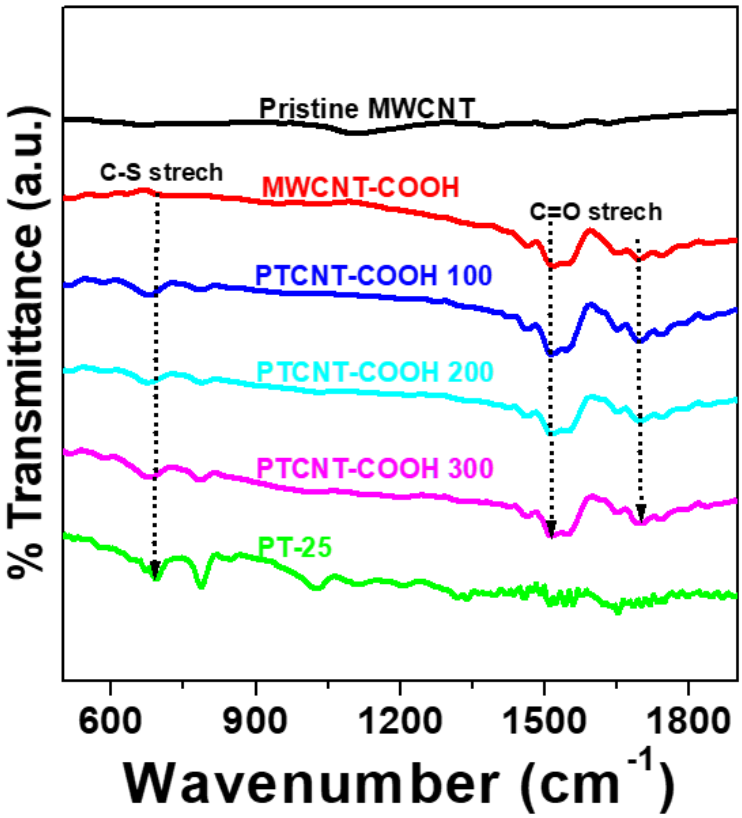

Figure 3.8. *FT-IR spectra of pristine MWCNT, MWCNT-COOH, PTCNT-COOH 100, PTCNT-COOH 200, PTCNT-COOH 300 and PT-25.*

The pH studies of aqueous dispersed forms of the samples such as functionalized MWCNT-COOH, PTCNT-COOH 100, PTCNT-COOH 200 and PTCNT-COOH 300 were carried out using a pH meter. The pH value of MWCNT-COOH was obtained as 4.8, which is acidic due to the dissociation of H^+ ion from carboxylic acid groups. The pH values of PTCNT-COOH 300, PTCNT-COOH 200 and PTCNT-COOH 100 gradually increased to 5.4, 6.2 and 6.7, respectively. This increase in pH (decrease in acidity) was attributed to the lesser amount of MWCNT-COOH added (300 to 100 mg) to each composite systems but not due to the suppression of dissociation of the hydrogen ions by the polythiophene layer. Therefore, free carboxylic acid groups on MWCNT-COOH make relatively more acidic, whereas in nanocomposites (PTCNT-COOHs) decrease in acidity was due to composite formation. Elemental analysis (CHNS analysis) was taken to analyze

the compositional ratio of carbon, hydrogen and sulfur present in the composites of PTCNT-COOH 100 and PTCNT-COOH 300. PTCNT-COOH 300 has a lesser compositional weight percentage of sulfur due to a higher proportion of CNT compared to that of PTCNT-COOH 100.

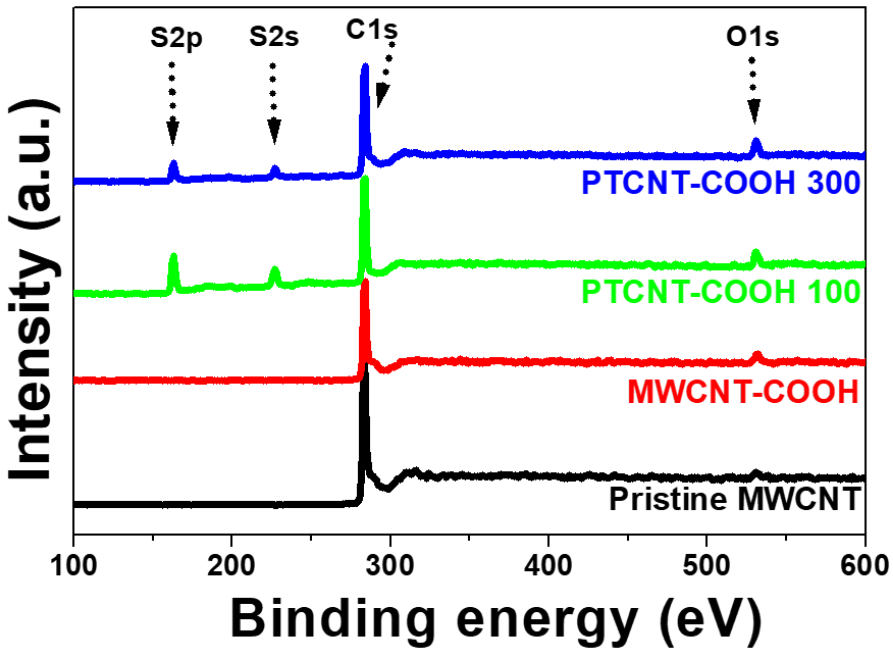

Figure 3.9. *XPS spectra of pristine MWCNT, MWCNT-COOH, PTCNT-COOH 100 and PTCNT-COOH 300.*

The X-ray photoelectron spectroscopy (XPS) was employed for the detailed elemental study of pristine MWCNT, functionalized MWCNT-COOH, PTCNT-COOH 100 and PTCNT-COOH 300 and to obtain an understanding of their functionalization ratio (see **Figure 3.9.**). Pristine MWCNT has shown an intense high peak at 283.25 eV and a very weak intensity peak at 531.45 eV corresponding to C 1s and O 1s, respectively. MWCNT-COOH exhibited an intense peak at 283.45 eV corresponding to C 1s and a relatively intense peak at 531.6 eV corresponding to O 1s. Furthermore, an enhancement in the XPS peak intensity was observed for the O 1s peak of functionalized MWCNT-COOH compared with pristine MWCNT, which attributes the formation of oxygen containing functional groups as defective sites. [43] Samples like PTCNT-COOH 100 and PTCNT-COOH 300 have their spectral profiles with characteristic peaks of sulfur at 226.95 (S 2s) and 162.75 (S 2p) eV in addition to C 1s and O 1s peaks, which confirms the presence of polythiophene in PTCNT-COOHs.[49,50] The PTCNT-COOH 100 nanocomposite contains a high polythiophene compositional

ratio, which was evident from its dominating sulphur peak intensity compared with PTCNT-COOH 300.

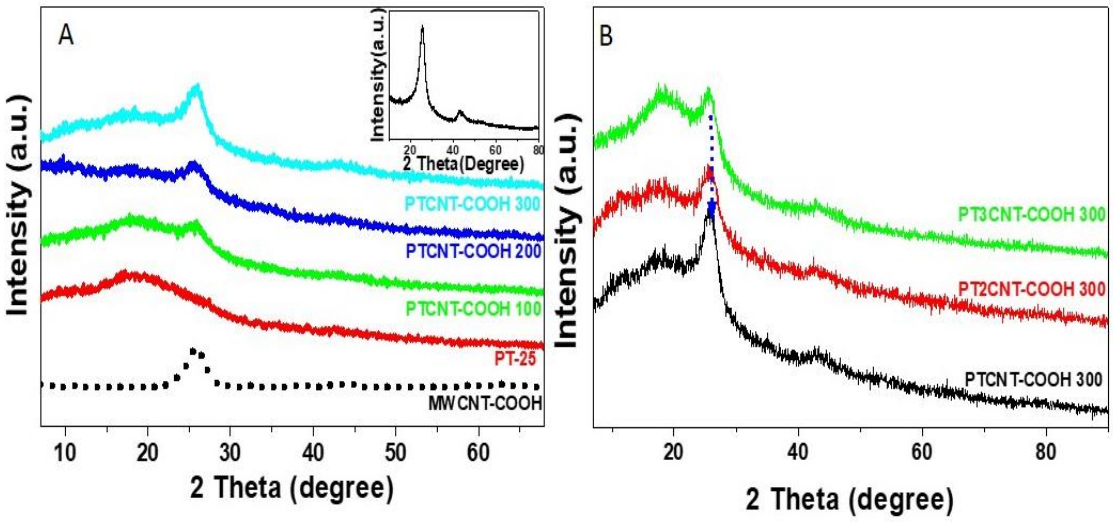

Figure 3.10. *Powder X-ray diffractograms of (A) MWCNT-COOH, PT-25, PTCNT-COOH 100, PTCNT-COOH 200, PTCNT-COOH 300 and pristine MWCNT (in inset). (B) Comparison of X-ray diffraction diagram of PTCNT-COOH 300, PT2CNT-COOH 300 and PT3CNT-COOH 300.*

X-ray diffractograms of functionalized MWCNT-COOH, polythiophene (PT), PTCNT-COOH 100, PTCNT-COOH 200 and PTCNT-COOH 300 have been analysed to understand the extent of solid-state packing of polymer matrix on CNT (see **Figure 3.10. A**). The functionalized MWCNT-COOH mainly exhibited an intense peak at 2θ value 25.85° attributing to the (002) diffraction plane of MWCNT having graphitic structure.[30,50] Typical polythiophene (PT) has the broad amorphous peak centered at 18.68°.[30,51] A Polythiophene-functionalized multi-walled carbon nanotube nanocomposites such as PTCNT-COOH 100, PTCNT-COOH 200 and PTCNT-COOH 300 exhibited a broad peak centered at 18.53° beside the (002) plane diffraction peak of carbon nanotube graphitic structure at 26.02°. On moving from PTCNT-COOH 100 to PTCNT-COOH 300, the intensity of broad amorphous peak of polythiophene goes down and the intensity of the (002) plane diffraction peak goes up. This result points out that PTCNT-COOH 300 provides more surface area on the CNT backbone compared to PTCNT-COOH 200 and PTCNT-COOH 100 for covering polythiophene nanolayer around the nanotube surface.[51-54] The low compositional ratio of thiophene in PTCNT-COOH 300 was reversed by increasing the thiophene monomer in feed (see

Figure 3.10. B for XRD pattern of PT2CNT-300 and PT3CNT-300). As the ratio of thiophene in feed increases on the CNT surface, the intensity of the amorphous polythiophene peak increases. X-ray diffraction patterns of polythiophene-CNT nanocomposites indicate that larger surface area of carbon nanotubes delivers more ordering in the polymer arrangement as nanolayer on CNT's surface.

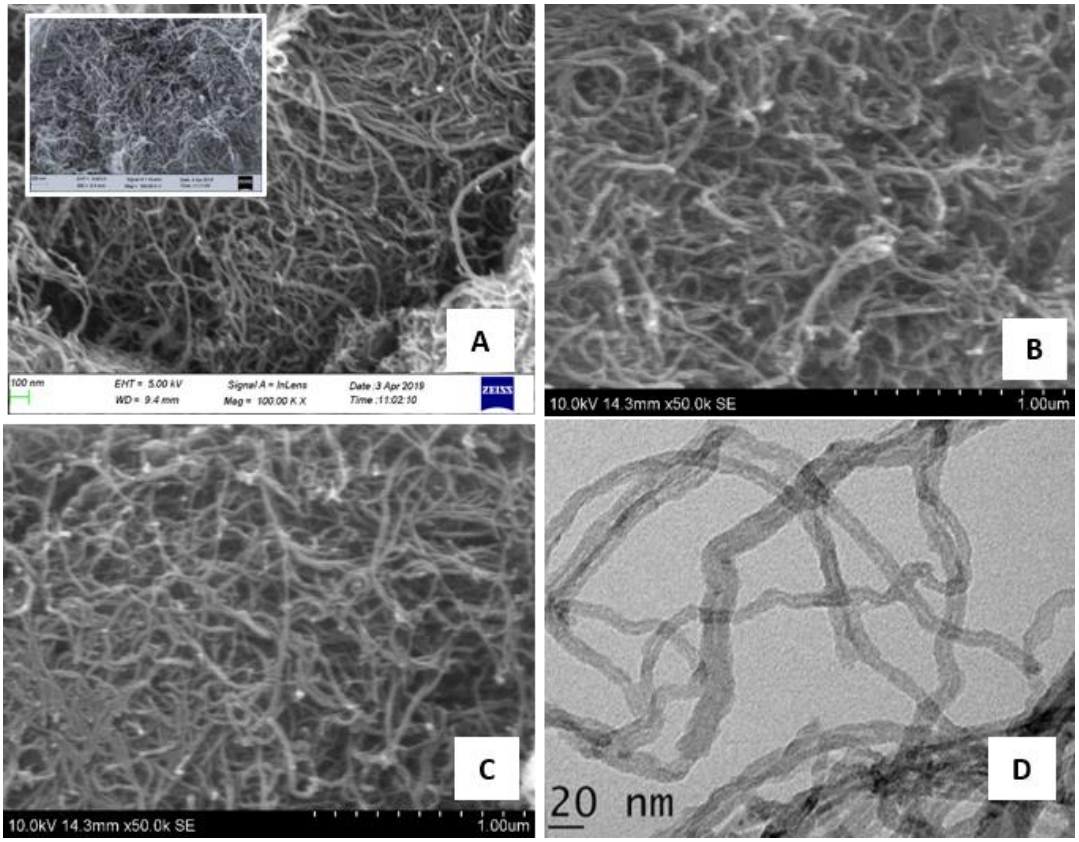

Figure 3.11. *FE-SEM images of (A) MWCNT-COOH, MWCNT (in inset), (B) PTCNT-COOH 100, (C) PTCNT-COOH 300 and (D) HR-TEM image of PTCNT-COOH 300*

The morphological characterisations of functionalized MWCNT-COOH and PTCNT-COOHs (100 and 300) were analysed using scanning electron microscopy (see **Figure 3.11.**). FE-SEM images of pristine MWCNT (inset of **Figure 3.11. A**) revealed its aggregated bundled nature, whereas surface oxidized MWCNT-COOH produced well separated carbon nanotubes after purification and washing (see **Figure 3.11. A**). These functionalized carbon nanotubes (MWCNT-COOH) could act as nano-tubular templates to accommodate in-situ formed polythiophene. The length of CNTs were not much cut shortened on acid treatment. In particular, binary nanocomposites such as PTCNT-COOH 300 composite have shown an increase in thickness without any phase separation (see **Figure 3.11. C**). Detailed morphological features and the inner

dimensions of the nanocomposite (PTCNT-COOH 300) have been investigated using transmission electron microscopy (TEM) (see **Figure 3.11. D**). TEM images revealed the remarkable thick outer layer having outer diameter of 14.80 ± 5 nm and inner tube diameter of 4.20 ± 2 nm. Higher outer to inner diameter ratio suggested that polythiophene was attached on the surface of the MWCNT as an outer layer through weak non-covalent interactions to form a thicker PT shell on the CNT core. An illustration of polythiophene chains orientation over MWCNT-COOH is represented in **Figure 3.12.**

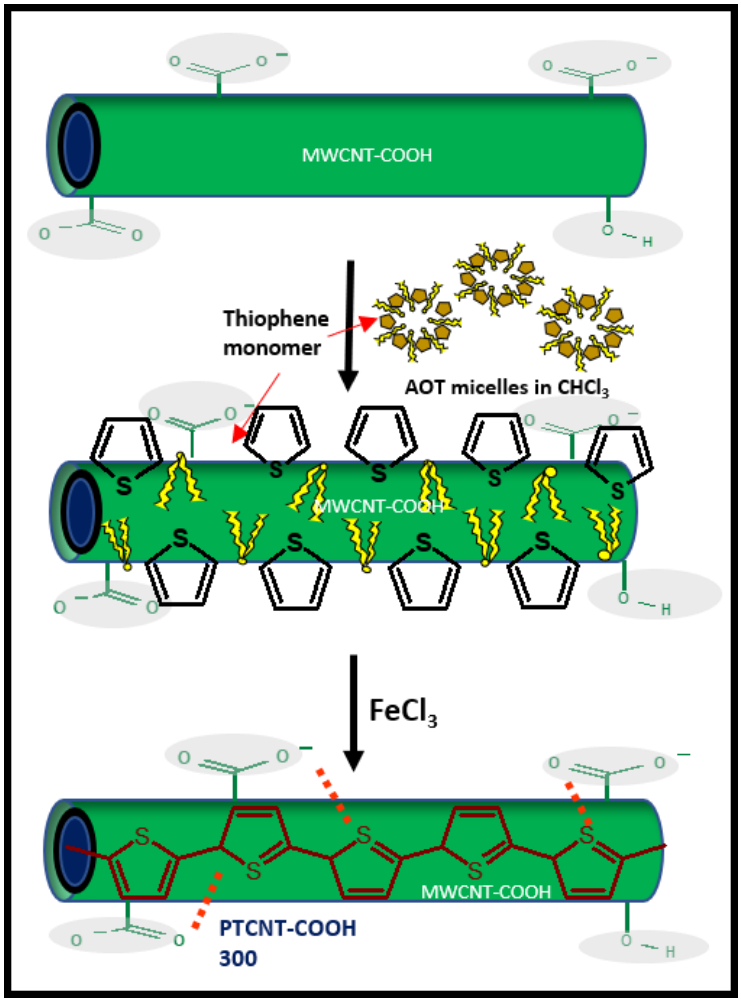

Figure 3.12. *Illustration of the utilisation of defect group functionalization for the orientation of polythiophene over MWCNT surface.*

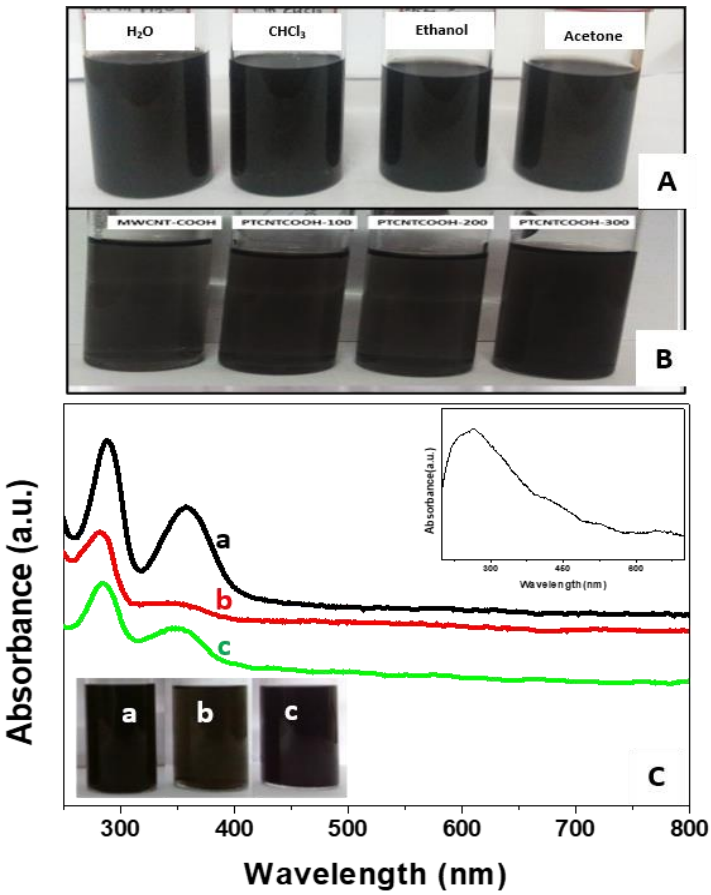

Figure 3.13. *Dispersion of MWCNT-COOH in different solvents (A) and aqueous dispersions of different nanocomposites (B). UV-vis spectra of PTCNT-COOH 100 in chloroform [a], PTCNT-COOH 300 in chloroform [b], PTCNT-COOH 300 in ethanol [c] and MWCNT-COOH in water [inset](C).*

The pristine multi-walled carbon nanotubes were usually insoluble in common solvents, mainly due to the bundling nature of carbon nanotubes and lack of functionalization. However, the covalent functionalization of multi-walled carbon nanotube by acid oxidation introduces polar groups such as carboxylic acid, hydroxyl and carbonyl groups which enhance the solubility, especially in polar solvents. The functionalised MWCNT-COOH covered with conducting polymers also reduces the bundling effect via repulsion between the tethered polymer chains creating an energy barrier against aggregation by controlling intertube potential.[52] Theoretical aspects of simulation study based on the interaction of conducting polymers with carbon nanotubes also communicate that those non-covalent interactions could better enhance the dispersibility and hence the processability.[53,54] Sonication of functionalized MWCNT-COOH and PTCNT-COOHs (100, 200 and 300) nanocomposites in water,

ethanol and chloroform have produced fairly stable dispersions (see **Figure 3.13. A** and **B**). The functionalized multi-walled carbon nanotubes (MWCNT-COOH) have shown absorption maximum at 260 nm due to aromatic π-π* absorption of carbon nanotube.[9,55] The UV-vis spectra of PTCNT-COOH 100 in chloroform and PTCNT-COOH 300 in ethanol and chloroform have shown well resolved peak at 360 nm in addition to a peak at 280 nm. The characteristic peak at 360 nm was due to polaron- π transition of polythiophene, which was intense for PTCNT-COOH 100.[9,55] The sample PTCNT-COOH 100 possesses less amount of functionalized MWCNT-COOH (100 mg) than PTCNT-COOH 300 (300 mg), therefore thick layer present in PTCNT-COOH-100 must have resulted in strong absorption of polaron transition (see **Figure 3.13. C**).[56]

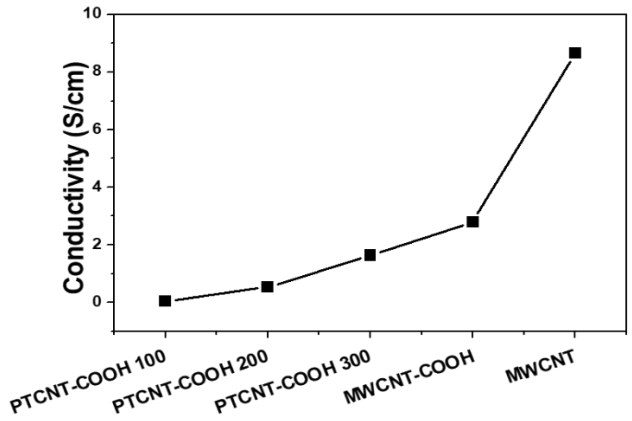

Figure 3.14. *Four probe electrical conductivity of PTCNT-COOH 100, PTCNT-COOH 200, PTCNT-COOH 300, MWCNT-COOH and pristine MWCNT.*

The electrical conductivities of pelletized pristine MWCNT, MWCNT-COOH, PTCNT-COOH 100, PTCNT-COOH 200 and PTCNT-COOH 300 were measured using four probe electrical conductivity meter (see **Figure 3.14.**). Electrical conductivities of pristine MWCNT, MWCNT-COOH, PTCNT-COOH 100, PTCNT-COOH-200 and PTCNT-COOH 300 measured were 8.66 S/cm, 2.80 S/cm, 4.42×10^{-2} S/cm, 5.30×10^{-1} S/cm and 1.64 S/cm respectively. Multi-walled carbon nanotubes exhibited a drop in electrical conductivity on acid functionalization. The decrease in electrical conductivity was due to the development of defective sites for functional group formation on the π-conjugated backbone.[57] Association of polythiophene with MWCNT-COOH also decreased the overall conductivity in nanocomposites (PTCNT-COOH 100, PTCNT-COOH 200 and PTCNT-COOH 300) due to the presence of high weight percentage of polythiophene which is individually less conducting than MWCNT. A comparison of the electrical conductivity of PTCNT-COOH with PTCNT

nanocomposites was given in **Table 3.3**. The electrical conductivities of both PTCNT-COOH and PTCNTs undergo increment with an increase in functionalized or non-functionalized carbon nanotubes. Among the nanocomposites with lesser carbon nanotube content, PTCNT-100 has better conductivity than PTCNT-COOH 100, whereas, in nanocomposites with higher carbon nanotube, PTCNT-COOH-200 and PTCNT-COOH-300 has better conductivity than PTCNT composites. The enhanced electrical conductivity of these polythiophene-functionalized carbon nanotube nanocomposites (PTCNT-COOH 200 and PTCNT-COOH 300) might be due to the effective electron transport between conducting polythiophene and carbon nanotubes within the well-formed core-shell nanostructure.[58,59] In addition to some of the non-covalent interactions present in PTCNT composites (discussed in Chapter 2), the formation of core shell morphology was furthermore reinforced in PTCNT-COOH composites by hydrogen bonding between functional groups formed on acid treatment and sulfur atoms in the polythiophene chains.

Table 3.3. *Comparison of conductivity values of PT-25, MWCNT, MWCNT-COOH, PTCNT and PTCNT-COOH nanocomposites*

Sample	Conductivity (S/cm)	Sample	Conductivity (S/cm)
PT-25	$7.3x10^{-3}$	-	-
PTCNT-100	3.58×10^{-1}	PTCNT-COOH 100	4.42×10^{-2}
PTCNT-200	3.98×10^{-1}	PTCNT-COOH 200	5.30×10^{-1}
PTCNT-400	3.40×10^{-1}	PTCNT-COOH 300	1.64
MWCNT	8.66	MWCNT-COOH	2.80

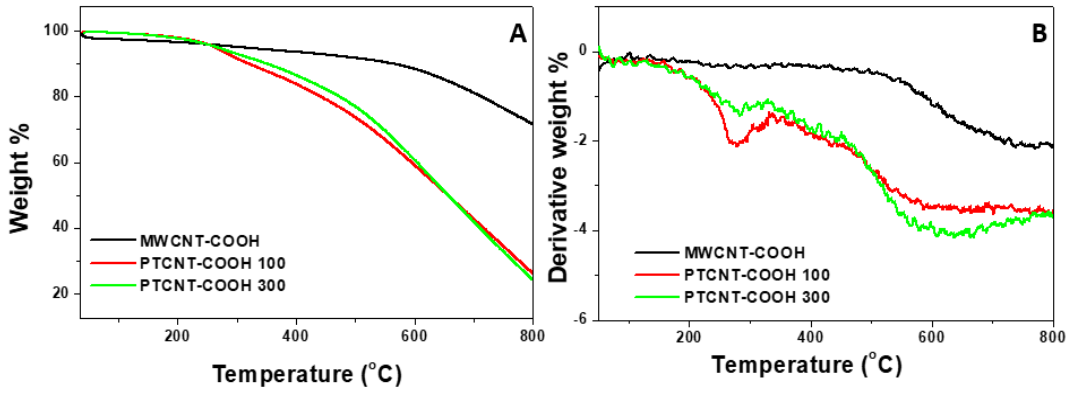

Figure 3.15. *TGA (A) and DTA (B) analysis of MWCNT-COOH, PTCNT-COOH 100 and PTCNT-COOH 300*

Thermal stability of MWCNT-COOH, PTCNT-COOH 100, PTCNT-COOH 300 were analysed in the scan rate of 20°C/min with nitrogen atmosphere (see **Figure 3.15.**). Functionalized MWCNT-COOH exhibited only 10% weight loss up to 620°C due to its graphitic network structure. PTCNT-COOH 100 and PTCNT-COOH 300 nanocomposites showed 10% weight loss up to 350°C. PTCNT-100 and PTCNT-300 nanocomposites (discussed in Chapter 2) exhibited approximately 15% weight loss up to 350°C. Therefore, PTCNT-COOH composites have shown comparably higher thermal stability than PTCNT composites up to 350°C. Thermal degradation up to this temperature was due to polymer degradation from the carbon chain. A better polymer interaction with a carbon nanotube via non-covalent interaction in PTCNT-COOH might have facilitated higher thermal stability than PTCNT nanocomposites. At higher temperature regions (beyond 400°C), the thermal degradation is due to the breakdown of the carbon nanotube structure. At this stage, PTCNTs have slightly better thermal stability than PTCNT-COOHs because the thermal degradation of MWCNT-COOH was faster than pristine MWCNT. Discrete stages of decomposition during the temperature scan were examined with differential thermal analysis. The decomposition of functionalized MWCNT-COOH was observed from 510°C with a one step decomposition. PTCNT-COOH 100 and PTCNT-COOH 300 were observed to decompose in two steps; starting from 260°C to 340˚C due to the degradation of polythiophene and the other one starting from 470˚C owes to the structural decomposition of CNT.[58,59]

The advantages of enhanced properties of PTCNT-COOH nanocomposites compared to individual components (MWCNT-COOH and polythiophene) can pave the way for utilisation of composite in numerous applications (see **Figure 3.16.**). The preparation of easily processable materials is a major area of research these days. Achievement of stable dispersion would create debundled carbon nanotubes in its composite structure, which further enhances the processability of the material when they are used in various applications. Stable aqueous dispersions would be more attractive than other dispersion mediums because the solvent water is accepted as universal and green solvent. The prepared nanocomposites PTCNT-COOHs have given stable dispersions in water or other polar solvents and have attractive properties like good electrical conductivity and thermal stability, with striking relevance in various applications.

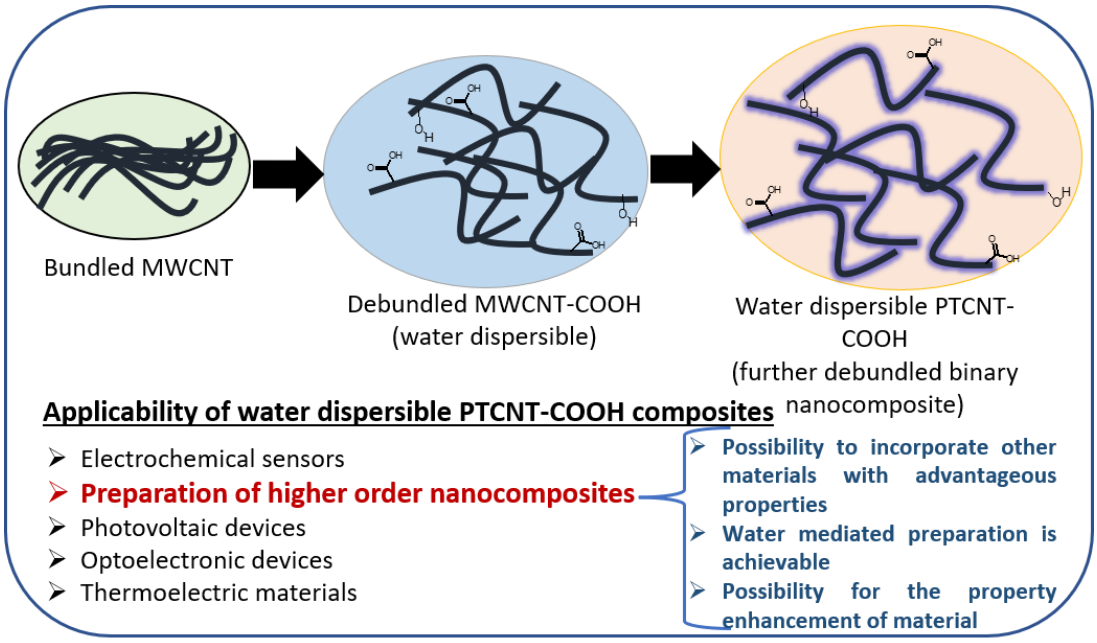

Figure 3.16. *Illustration of debundling effect of carbon nanotubes by carboxylic acid functionalization followed by non-covalent functionalization with polymer*

3.4. Conclusion

In a nutshell, polythiophene-functionalized carbon nanotube nanocomposites (PTCNT-COOHs) were synthesised by in-situ chemical oxidative polymerisation of thiophene monomer using ferric chloride as oxidising agent in the dispersion of functionalized MWCNT-COOH in chloroform and AOT as the surfactant. Functionalized MWCNT-COOH was prepared by refluxing with 5 M nitric acid. The formation of polythiophene-MWCNT-COOH composite was primarily ascertained with fourier transform Infrared spectra and X-ray photoelectron spectroscopy. The pH studies indicated the acidic nature of MWCNT- COOH and PTCNT-COOHs due to presence of carboxyl acid functional groups on the CNT surface. X-ray photoelectron spectroscopic peaks confirmed the functionalization of MWCNT-COOH with oxygen containing functional groups and presence of polythiophene in PTCNT-COOH nanocomposites. The variation in XPS peak intensity shows the proportional correlation between polymer and CNT components in PTCNT-COOH composites. X-ray diffractograms revealed the formation of polythiophene nanolayer on the MWCNT-

COOH surface via non-bonding interactions like π-π stacking assembling and hydrogen bonding interactions. Field emission scanning electron microscopic images revealed the nanotubular morphology of PTCNT nanocomposites as same as that of multi-walled carbon nanotubes, but with more thickened walls on nanocomposite. The thicker outer tube diameter of PTCNT-COOH 300 was measured as 14.80 ± 5 nm by TEM analysis. Polythiophene chains in ordered arrangement on MWCNT-COOH walls were established as an energy barrier against tubular aggregation. The well dispersed state of MWCNT-COOH and PTCNT-COOHs in less aggregated form has given well-resolved peaks for UV-visible absorption spectra in water and ethanol medium. PTCNT-COOH nanocomposites were also found to be exhibited good electrical conductivity up to the order of 10^{-1} S/cm and good enough thermal stability up to 480°C. PTCNT-COOH composites have high dispersibility in green solvent water and other properties suitable for various applications.

References

1. T. A. Skotheim, J. R. Reynolds, Conjugated Polymers. Theory, Synthesis, Properties and Characterization (2007).
2. Spitalsky, Z.; Tasis, D.; Papagelis, K.; Galiotis, C. Carbon Nanotube-Polymer Composites: Chemistry, Processing, Mechanical and Electrical Properties. *Prog. Polym. Sci.* **2010**, *35* (3), 357–401. https://doi.org/10.1016/j.progpolymsci.2009.09.003.
3. Shirakawa, H. The Discovery of Polyacetylene Film: The Dawning of an Era of Conducting Polymers (Nobel Lecture). *Angew. Chemie - Int. Ed.* **2001**, *40* (14), 2574–2580. https://doi.org/10.1002/1521-3773(20010716)40:14<2574::aid-anie2574>3.0.co;2-n.
4. Guldi, D. M.; Rahman, G. M. A.; Zerbetto, F.; Prato, M. Carbon Nanotubes in Electron Donor - Acceptor Nanocomposites. *Acc. Chem. Res.* **2005**, *38* (11), 871–878. https://doi.org/10.1021/ar040238i.
5. Gong, X.; Liu, J.; Baskaran, S.; Voise, R. D.; Young, J. S. Surfactant-Assisted Processing of Carbon Nanotube/Polymer Composites. *Chem. Mater.* **2000**, *12* (4), 1049–1052. https://doi.org/10.1021/cm9906396.
6. Chen, W. C.; Lien, H. T.; Cheng, T. W.; Su, C.; Chong, C. W.; Ganguly, A.; Chen, K. H.; Chen, L. C. Side Group of Poly(3-Alkylthiophene)s Controlled Dispersion of Single-Walled Carbon Nanotubes for Transparent Conducting Film. *ACS Appl. Mater. Interfaces* **2015**, *7* (8), 4616–4622. https://doi.org/10.1021/am507774c.
7. C. Zhan, G. Yu, Y. Lu, L. Wang, E. Wujcik, S. Wei, Conductive polymer nanocomposites: a critical review of modern advanced devices, J. Mater. Chem. C. 5 (**2017**), 5 1569–1585. doi:10.1039/c6tc04269d.
8. Miller, A. J.; Hatton, R. A.; Silva, S. R. P. Water-Soluble Multiwall-Carbon-Nanotube-Polythiophene Composite for Bilayer Photovoltaics. *Appl. Phys. Lett.* **2006**, *89* (12). https://doi.org/10.1063/1.2356115.
9. Miller, A. J.; Hatton, R. A.; Silva, S. R. P. Water-Soluble Multiwall-Carbon-Nanotube-Polythiophene Composite for Bilayer Photovoltaics. *Appl. Phys. Lett.* **2006**, *89* (12). https://doi.org/10.1063/1.2356115.
10. Koval'chuk, A. A.; Shchegolikhin, A. N.; Shevchenko, V. G.; Nedorezova, P. M.; Klyamkina, A. N.; Aladyshev, A. M. Synthesis and Properties of Polypropylene/Multiwall

Carbon Nanotube Composites. *Macromolecules* **2008**, *41* (9), 3149–3156. https://doi.org/10.1021/ma800297e.
11. Mondal, R. K.; Dubey, K. A.; Bhardwaj, Y. K. Role of the Interface on Electron Transport in Electro-Conductive Polymer-Matrix Composite: A Review. *Polym. Compos.* **2021**, *42* (6), 2614–2628. https://doi.org/10.1002/pc.26018.
12. Berger, F. J.; Lüttgens, J.; Nowack, T.; Kutsch, T.; Lindenthal, S.; Kistner, L.; Müller, C. C.; Bongartz, L. M.; Lumsargis, V. A.; Zakharko, Y.; Zaumseil, J. Brightening of Long, Polymer-Wrapped Carbon Nanotubes by Sp3 Functionalization in Organic Solvents. *ACS Nano* **2019**, *13* (8), 9259–9269. https://doi.org/10.1021/acsnano.9b03792.
13. Hill, D. E.; Lin, Y.; Rao, A. M.; Allard, L. F.; Sun, Y. P. Functionalization of Carbon Nanotubes with Polystyrene. *Macromolecules* **2002**, *35* (25), 9466–9471. https://doi.org/10.1021/ma020855r.
14. Yu, H.; Jin, Y.; Peng, F.; Wang, H.; Yang, J. Kinetically Controlled Side-Wall Functionalization of Carbon Nanotubes by Nitric Acid Oxidation. *J. Phys. Chem. C* **2008**, *112* (17), 6758–6763. https://doi.org/10.1021/jp711975a.
15. Palacin, T.; Le Khanh, H.; Jousselme, B.; Jegou, P.; Filoramo, A.; Ehli, C.; Guldi, D. M.; Campidelli, S. Efficient Functionalization of Carbon Nanotubes with Porphyrin Dendrons via Click Chemistry. *J. Am. Chem. Soc.* **2009**, *131* (42), 15394–15402. https://doi.org/10.1021/ja906020e.
16. Dyke, C. A.; Tour, J. M. Covalent Functionalization of Single-Walled Carbon Nanotubes for Materials Applications. *J. Phys. Chem. A* **2004**, *108* (51), 11151–11159. https://doi.org/10.1021/jp046274g.
17. Kong, H.; Gao, C.; Yan, D. Controlled Functionalization of Multiwalled Carbon Nanotubes by in Situ Atom Transfer Radical Polymerization. *J. Am. Chem. Soc.* **2004**, *126* (2), 412–413. https://doi.org/10.1021/ja0380493.
18. Chen, R. J.; Zhang, Y.; Wang, D.; Dai, H. Noncovalent Sidewall Functionalization of Single-Walled Carbon Nanotubes for Protein Immobilization [11]. *J. Am. Chem. Soc.* **2001**, *123* (16), 3838–3839. https://doi.org/10.1021/ja010172b.
19. Clavé, G.; Delport, G.; Roquelet, C.; Lauret, J. S.; Deleporte, E.; Vialla, F.; Langlois, B.; Parret, R.; Voisin, C.; Roussignol, P.; Jousselme, B.; Gloter, A.; Stephan, O.; Filoramo, A.; Derycke, V.; Campidelli, S. Functionalization of Carbon Nanotubes through Polymerization in Micelles: A Bridge between the Covalent and Noncovalent Methods. *Chem. Mater.* **2013**, *25* (13), 2700–2707. https://doi.org/10.1021/cm401312v.
20. Simmons, T. J.; Bult, J.; Hashim, D. P.; Linhardt, R. J.; Ajayan, P. M. Noncovalent Functionalization as an Alternative to Oxidative Acid Treatment of Single Wall Carbon Nanotubes with Applications for Polymer Composites. *ACS Nano* **2009**, *3* (4), 865–870. https://doi.org/10.1021/nn800860m.
21. Wang, S. Optimum Degree of Functionalization for Carbon Nanotubes. *Curr. Appl. Phys.* **2009**, *9* (5), 1146–1150. https://doi.org/10.1016/j.cap.2009.01.004.
22. Buffa, F.; Hu, H.; Resasco, D. E. Side-Wall Functionalization of Single-Walled Carbon Nanotubes with 4-Hydroxymethylaniline Followed by Polymerization of ε-Caprolactone. *Macromolecules* **2005**, *38* (20), 8258–8263. https://doi.org/10.1021/ma050876w.
23. Lourenço, M. A. O.; Fontana, M.; Jagdale, P.; Pirri, C. F.; Bocchini, S. Improved CO2 Adsorption Properties through Amine Functionalization of Multi-Walled Carbon Nanotubes. *Chem. Eng. J.* **2021**, *414*, 128763. https://doi.org/10.1016/j.cej.2021.128763.
24. Bilalis, P.; Katsigiannopoulos, D.; Avgeropoulos, A.; Sakellariou, G. Non-Covalent Functionalization of Carbon Nanotubes with Polymers. *RSC Adv.* **2014**, *4* (6), 2911–2934. https://doi.org/10.1039/c3ra44906h.
25. Bose, S.; Khare, R. A.; Moldenaers, P. Assessing the Strengths and Weaknesses of Various Types of Pre-Treatments of Carbon Nanotubes on the Properties of Polymer/Carbon Nanotubes Composites: A Critical Review. *Polymer (Guildf).* **2010**, *51* (5), 975–993. https://doi.org/10.1016/j.polymer.2010.01.044.

26. Yuan, W.; Chan-Park, M. B. Covalent Cum Noncovalent Functionalizations of Carbon Nanotubes for Effective Reinforcement of a Solution Cast Composite Film. *ACS Appl. Mater. Interfaces* **2012**, *4* (4), 2065–2073. https://doi.org/10.1021/am300038d.
27. Kainz, Q. M.; Schätz, A.; Zöpfl, A.; Stark, W. J.; Reiser, O. Combined Covalent and Noncovalent Functionalization of Nanomagnetic Carbon Surfaces with Dendrimers and BODIPY Fluorescent Dye. *Chem. Mater.* **2011**, *23* (16), 3606–3613. https://doi.org/10.1021/cm200705d.
28. Bahr, J. L.; Yang, J.; Kosynkin, D. V.; Bronikowski, M. J.; Smalley, R. E.; Tour, J. M. Functionalization of Carbon Nanotubes by Electrochemical Reduction of Aryl Diazonium Salts: A Bucky Paper Electrode. *J. Am. Chem. Soc.* **2001**, *123* (27), 6536–6542. https://doi.org/10.1021/ja010462s.
29. Peng, H.; Alemany, L. B.; Margrave, J. L.; Khabashesku, V. N. Sidewall Carboxylic Acid Functionalization of Single-Walled Carbon Nanotubes. *J. Am. Chem. Soc.* **2003**, *125* (49), 15174–15182. https://doi.org/10.1021/ja037746s.
30. Lin, Y.; Zhou, B.; Fernando, K. A. S.; Liu, P.; Allard, L. F.; Sun, Y. P. Polymeric Carbon Nanocomposites from Carbon Nanotubes Functionalized with Matrix Polymer. *Macromolecules* **2003**, *36* (19), 7199–7204. https://doi.org/10.1021/ma0348876.
31. Ying, Y.; Saini, R. K.; Liang, F.; Sadana, A. K.; Billups, W. E. Functionalization of Carbon Nanotubes by Free Radicals. *Org. Lett.* **2003**, *5* (9), 1471–1473. https://doi.org/10.1021/ol0342453.
32. Lin, Y.; Zhou, B.; Martin, R. B.; Henbest, K. B.; Harruff, B. A.; Riggs, J. E.; Guo, Z. X.; Allard, L. F.; Sun, Y. P. Visible Luminescence of Carbon Nanotubes and Dependence on Functionalization. *J. Phys. Chem. B* **2005**, *109* (31), 14779–14782. https://doi.org/10.1021/jp053073j.
33. Khare, B.; Wilhite, P.; Tran, B.; Teixeira, E.; Fresquez, K.; Mvondo, D. N.; Bauschlicher, C.; Meyyappan, M. Functionalization of Carbon Nanotubes via Nitrogen Glow Discharge. *J. Phys. Chem. B* **2005**, *109* (49), 23466–23472. https://doi.org/10.1021/jp0537254.
34. Yang, D. Q.; Rochette, J. F.; Sacher, E. Controlled Chemical Functionalization of Multiwalled Carbon Nanotubes by Kiloelectronvolt Argon Ion Treatment and Air Exposure. *Langmuir* **2005**, *21* (18), 8539–8545. https://doi.org/10.1021/la0514922.
35. Hill, D.; Lin, Y.; Qu, L.; Kitaygorodskiy, A.; Connell, J. W.; Allard, L. F.; Sun, Y. P. Functionalization of Carbon Nanotubes with Derivatized Polyimide. *Macromolecules* **2005**, *38* (18), 7670–7675. https://doi.org/10.1021/ma0509210.
36. Hou, Y.; Tang, J.; Zhang, H.; Qian, C.; Feng, Y.; Liu, J. Functionalized Few-Walled Carbon Nanotubes for Mechanical Reinforcement of Polymeric Composites. *ACS Nano* **2009**, *3* (5), 1057–1062. https://doi.org/10.1021/nn9000512.
37. Chen, C.; Liang, B.; Ogino, A.; Wang, X.; Nagatsu, M. Oxygen Functionalization of Multiwall Carbon Nanotubes by Microwave-Excited Surface-Wave Plasma Treatment. *J. Phys. Chem. C* **2009**, *113* (18), 7659–7665. https://doi.org/10.1021/jp9012015.
38. Lerner, M. B.; D'Souza, J.; Pazina, T.; Dailey, J.; Goldsmith, B. R.; Robinson, M. K.; Johnson, A. T. C. Hybrids of a Genetically Engineered Antibody and a Carbon Nanotube Transistor for Detection of Prostate Cancer Biomarkers. *ACS Nano* **2012**, *6* (6), 5143–5149. https://doi.org/10.1021/nn300819s.
39. Likodimos, V.; Steriotis, T. A.; Papageorgiou, S. K.; Romanos, G. E.; Marques, R. R. N.; Rocha, R. P.; Faria, J. L.; Pereira, M. F. R.; Figueiredo, J. L.; Silva, A. M. T.; Falaras, P. Controlled Surface Functionalization of Multiwall Carbon Nanotubes by HNO3 Hydrothermal Oxidation. *Carbon N. Y.* **2014**, *69*, 311–326. https://doi.org/10.1016/j.carbon.2013.12.030.
40. Osswald, S.; Havel, M.; Gogotsi, Y. Monitoring Oxidation of Multiwalled Carbon Nanotubes by Raman Spectroscopy. *J. Raman Spectrosc.* **2007**, *38* (6), 728–736. https://doi.org/10.1002/jrs.1686.
41. Avilés, F.; Cauich-Rodríguez, J. V.; Moo-Tah, L.; May-Pat, A.; Vargas-Coronado, R. Evaluation of Mild Acid Oxidation Treatments for MWCNT Functionalization. *Carbon N. Y.* **2009**, *47* (13), 2970–2975. https://doi.org/10.1016/j.carbon.2009.06.044.

42. Osorio, A. G.; Silveira, I. C. L.; Bueno, V. L.; Bergmann, C. P. H 2 SO 4 /HNO 3 /HCl-Functionalization and Its Effect on Dispersion of Carbon Nanotubes in Aqueous Media. *Appl. Surf. Sci.* **2008**, *255* (5 PART 1), 2485–2489. https://doi.org/10.1016/j.apsusc.2008.07.144.
43. Stobinski, L.; Lesiak, B.; Kövér, L.; Tóth, J.; Biniak, S.; Trykowski, G.; Judek, J. Multiwall Carbon Nanotubes Purification and Oxidation by Nitric Acid Studied by the FTIR and Electron Spectroscopy Methods. *J. Alloys Compd.* **2010**, *501* (1), 77–84. https://doi.org/10.1016/j.jallcom.2010.04.032.
44. Swathy, T. S.; Jose, M. A.; Antony, M. J. AOT Assisted Preparation of Ordered, Conducting and Dispersible Core-Shell Nanostructured Polythiophene – MWCNT Nanocomposites. *Polymer (Guildf).* **2016**, *103*, 206–213. https://doi.org/10.1016/j.polymer.2016.09.047.
45. Jinish Antony, M.; Albin Jolly, C.; Rohini Das, K.; Swathy, T. S. Normal and Reverse AOT Micelles Assisted Interfacial Polymerization for Polyaniline Nanostructures. *Colloids Surfaces A Physicochem. Eng. Asp.* **2019**, *578*, 123627. https://doi.org/10.1016/j.colsurfa.2019.123627.
46. M. A. Jose, S. Varghese, Antony M. J. *In situ* chemical oxidative polymerisation for ordered conducting polythiophene nanostructures in presence of dioctyl sodium sulfosuccinate, IJC-A 55A (2016) 291-297.
47. R. Liu, Z. Liu, Polythiophene: Synthesis in aqueous medium and controllable morphology, Sci. Bull. 54 (2009), *54*, 2028–2032. doi:10.1007/s11434-009-0217-0.
48. Gök, A.; Omastová, M.; Yavuz, A. G. Synthesis and Characterization of Polythiophenes Prepared in the Presence of Surfactants. *Synth. Met.* **2007**, *157* (1), 23–29. https://doi.org/10.1016/j.synthmet.2006.11.012.
49. Dabera, G. D. M. R.; Jayawardena, K. D. G. I.; Prabhath, M. R. R.; Yahya, I.; Tan, Y. Y.; Nismy, N. A.; Shiozawa, H.; Sauer, M.; Ruiz-Soria, G.; Ayala, P.; Stolojan, V.; Adikaari, A. A. D. T.; Jarowski, P. D.; Pichler, T.; Silva, S. R. P. Hybrid Carbon Nanotube Networks as Efficient Hole Extraction Layers for Organic Photovoltaics. *ACS Nano* **2013**, *7* (1), 556–565. https://doi.org/10.1021/nn304705t.
50. Cao, A.; Xu, C.; Liang, J.; Wu, D.; Wei, B. X-Ray Diffraction Characterization on the Alignment Degree of Carbon Nanotubes. *Chem. Phys. Lett.* **2001**, *344* (1–2), 13–17. https://doi.org/10.1016/S0009-2614(01)00671-6.
51. Senthilkumar, B.; Thenamirtham, P.; Kalai Selvan, R. Structural and Electrochemical Properties of Polythiophene. *Appl. Surf. Sci.* **2011**, *257* (21), 9063–9067. https://doi.org/10.1016/j.apsusc.2011.05.100.
52. Shvartzman-Cohen, R.; Nativ-Roth, E.; Baskaran, E.; Levi-Kalisman, Y.; Szleifer, I.; Yerushalmi-Rozen, R. Selective Dispersion of Single-Walled Carbon Nanotubes in the Presence of Polymers: The Role of Molecular and Colloidal Length Scales. *J. Am. Chem. Soc.* **2004**, *126* (45), 14850–14857. https://doi.org/10.1021/ja046377c.
53. Hooper, J. B.; Schweizer, K. S. Theory of Phase Separation in Polymer Nanocomposites. *Macromolecules* **2006**, *39* (15), 5133–5142. https://doi.org/10.1021/ma060577m.
54. Tummala, N. R.; Morrow, B. H.; Resasco, D. E.; Striolo, A. Stabilization of Aqueous Carbon Nanotube Dispersions Using Surfactants: Insights from Molecular Dynamics Simulations. *ACS Nano* **2010**, *4* (12), 7193–7204. https://doi.org/10.1021/nn101929f.
55. Ago, H.; Kugler, T.; Cacialli, F.; Salaneck, W. R.; Shaffer, M. S. P.; Windle, A. H.; Friend, R. H. Work Functions and Surface Functional Groups of Multiwall Carbon Nanotubes. *J. Phys. Chem. B* **1999**, *103* (38), 8116–8121. https://doi.org/10.1021/jp991659y.
56. Liang, L.; Xie, W.; Fang, S.; He, F.; Yin, B.; Tlili, C.; Wang, D.; Qiu, S.; Li, Q. High-Efficiency Dispersion and Sorting of Single-Walled Carbon Nanotubes: Via Non-Covalent Interactions. *J. Mater. Chem. C* **2017**, *5* (44), 11339–11368. https://doi.org/10.1039/c7tc04390b.
57. Razavi, R.; Zare, Y.; Rhee, K. Y. A Two-Step Model for the Tunneling Conductivity of Polymer Carbon Nanotube Nanocomposites Assuming the Conduction of Interphase Regions. RSC Adv. 2017, 7 (79), 50225–50233. https://doi.org/10.1039/c7ra08214b.

58. Kuila, B. K.; Malik, S.; Batabyal, S. K.; Nandi, A. K. In-Situ Synthesis of Soluble Poly(3-Hexylthiophene)/Multiwalled Carbon Nanotube Composite: Morphology, Structure, and Conductivity. Macromolecules 2007, 40 (2), 278–287. https://doi.org/10.1021/ma061548e.
59. Saini, V.; Li, Z.; Bourdo, S.; Dervishi, E.; Xu, Y.; Ma, X.; Kunets, V. P.; Salamo, G. J.; Viswanathan, T.; Biris, A. R.; Saini, D.; Biris, A. S. Electrical, Optical, and Morphological Properties of P3ht-Mwnt Nanocomposites Prepared by In Situ Polymerization. J. Phys. Chem. C 2009, 113 (19), 8023–8029. https://doi.org/10.1021/jp809479a.